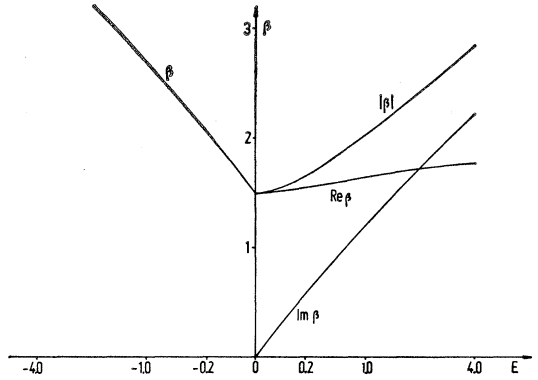

FIG. 18. The parameter $\beta(E+i0)$, as given by Eq. (B.7); again, $\mu=m=\lambda=1$.

nator is calculated in $\mathbf{x}$ space, making use of the locality of $V(r)$ to form $V^{-1}(r)$. We thus obtain

$$[\eta(E)]=\lambda(2\beta-\mu)^2/2\beta(\beta-iE^{1/2})^2. \quad \text{(B6)}$$

This becomes a maximum if

$$\beta(E)=\tfrac{3}{4}\mu-\tfrac{1}{2}(iE^{1/2})+\tfrac{1}{2}(9\mu^2/4-5i\mu E^{1/2}-E)^{1/2}. \quad \text{(B7)}$$

$\eta(E)$ and $\beta(E)$ are shown in Figs. 17 and 18. There we see that the imaginary parts both of β and of η soon become very important if one goes to positive energies. Looking at $E=0$, and using (B4) and (3.3), we find $\xi(0)=8/7$, which is indeed rather close to unity, as was suggested by the arguments leading to our ansatz (3.10). At this energy ($E=0$), we obtained the Schmidt norms (see also Ref. 9)

$$\tau(0)=|G_0^{1/2}(0)V_0(0)G_0^{1/2}(0)|=\lambda(2\ln 2-1)^{1/2}=0.6215\lambda$$

and

$$\tau'(0)=|G_0^{1/2}(0)V_0'(0)G_0^{1/2}(0)|$$
$$=\{\tau^2(0)-2\langle\chi|G_0(0)VG_0(0)|\chi\rangle+[\eta(0)]^2\}^{1/2}.$$

The term $\langle\chi|G_0V_0G_0|\chi\rangle$, calculated in configuration space,[40] is

$$\langle\chi|G_0(0)VG_0(0)|\chi\rangle=\frac{2\lambda\mu}{\beta(0)}[\eta(0)]\ln\frac{(\mu+\beta)^2}{(\mu+2\beta)\mu},$$

which gives

$$\tau'(0)=0.1795\lambda.$$

The work of Weinberg and collaborators[9,40] shows that this is sufficient to make V^{sep} a very good approximation to V, if the coupling constant λ is not too large. Since in the three-nucleon problem a similar weakening of the potentials is achieved by subtraction of separable terms (see the results given in Sec. 4), we may expect that these separable terms represent a good approximation for our problem.

[40] M. Scadron and S. Weinberg, Phys. Rev. **133**, B1589 (1964).

PHYSICAL REVIEW C VOLUME 1, NUMBER 1 JANUARY 1970

New Statistical Theory of the Nuclear Surface. I*

PHILIP J. SIEMENS†
Laboratory of Nuclear Studies, Cornell University, Ithaca, New York

(Received 10 September 1969)

The Thomas-Fermi integral theory of the nuclear surface is shown to have singular solutions for the nuclear density. This failure is traced to its inadequate representation of the behavior of wave functions in a potential. A new theory based on approximate wave functions is developed and shown to be asymptotic to the Thomas-Fermi theory in the interior of the nucleus. An improved treatment of exchange forces is shown to be essential to obtaining realistic solutions.

I. INTRODUCTION

PREVIOUS statistical theories[1–3] of the nuclear surface have been formulated as variational problems in which the total energy W_T of a nucleus is minimized as a functional of its neutron and proton density distributions $\rho_n(\mathbf{r})$ and $\rho_p(\mathbf{r})$. The most thorough formulation of the problem is that of Bethe,[1] who writes W_T as an integral of the long-range direct force between nucleons, plus local-density approximations to the short-range force, the space-exchange integral, and the kinetic energy. Buchler *et al.*[2] approximate the long-range direct-force integral by a differential term, a fair approximation if the surface thickness is not too small; such a term includes the first-order correction of Weiszacker for the additional kinetic energy necessary to cause a varying density. In Sec. II, it is shown that the integral theory of Bethe can have discontinuous solutions. Such a solution is obtained numerically for the one-dimensional case. This singularity demonstrates that the surface thickness is due not only to the properties of the long-range direct nucleon-nucleon force, as argued by Wilets[3] and

* Work supported in part by the National Science Foundation.
† National Science Foundation Graduate Fellow.
[1] H. A. Bethe, Phys. Rev. **167**, 879 (1968).
[2] J. R. Buchler, R. J. Lombard, S. Jorna, and K. A. Brueckner, Phys. Rev. **171**, 1188 (1968).
[3] L. Wilets, Phys. Rev. **101**, 1805 (1956); R. A. Berg and L. Wilets, *ibid.* **101**, 201 (1956); L. Wilets, Rev. Mod. Phys. **30**, 542 (1958).

Bethe[1], but also to the necessity of the wave functions to anticipate the disappearance of the potential in which they move, before they reach the region of their classical turning points. In Sec. II, it is also shown that a continuous solution of the Thomas-Fermi equation would have much too low a central density—approximately that at which the nuclear-matter chemical potential has its minimum.

In Sec. III, an improved theory based on approximate wave functions is derived. This section extends the work of Kohn and Sham[4] to the case of a three-dimensional wave function in a potential which is a function of only one of the three Cartesian coordinates. The resulting relation between the potential and the Dirac mixed density rapidly approaches the local-density relation inside the nucleus, but differs in the surface.

Section IV applies the theory of Sec. III to the surface of the nucleus. It is shown that there is a large inhomogeneity correction to the single-particle potential due to the space-exchange part of the nuclear force. This exchange correction makes possible the achievement of solutions with an acceptable central density. In Sec. V, numerical results are discussed, but no solutions are obtained. Recent nuclear-matter results[5] are incorporated into the theory.

II. FAILURE OF THE THOMAS-FERMI THEORY

A. Thomas-Fermi Theory of Bethe

Bethe[1] obtains his Thomas-Fermi theory of nuclei by supposing that the total energy of a nucleus is given by[6]

$$W_T=\int d^3\mathbf{r}\, W(\rho)\rho(\mathbf{r})-(1+2\kappa)^{-1}\tfrac{1}{2}\int d^3\mathbf{r}\int d^3\mathbf{r}'\rho(\mathbf{r}) \times\{\rho(\mathbf{r})g_D(\mathbf{r}-\mathbf{r}',\rho(\mathbf{r})) -\rho(\mathbf{r}')g_D(\mathbf{r}-\mathbf{r}',\tfrac{1}{2}[\rho(\mathbf{r})+\rho(\mathbf{r}')])\}. \quad (2.1)$$

Here $W(\rho)$ is the binding energy per particle of nuclear matter at density ρ. The first term is thus merely the integral of the energy density of a Fermi gas of nucleons; it would be the only contribution to the energy if the range of the forces were very short compared to the distances over which the density varies. In the surface of a nucleus, however, these two distances are comparable. Therefore, it is necessary to add the second term, which is an inhomogeneity correction due to the long-range interaction between nucleons, g_D. The subscript D here means that only the ordinary, i.e., non-space-exchange, part of the force is to be used, since this is the part whose contribution to the energy is proportional to the product of the ordinary densities, $\rho(\mathbf{r})\rho(\mathbf{r}')g_D(\mathbf{r}-\mathbf{r}')$. g_D is assumed to depend on the density; this is necessary primarily because the force includes a strong contribution from a long-range tensor force, which depends strongly on the density.[5] The factor $1/(1+2\kappa)$ is a correction for self-consistency arising from Brueckner theory, as explained by Bethe[1]; κ is the dimensionless "wound integral" of that theory.

Thus, in Eq. (2.1), almost all the complicated features of the nuclear force, including the short-range correlations of Brueckner theory and the space-exchange part of the interaction, are absorbed into the nuclear-matter term $W(\rho)$. This is a very convenient way to treat the short-range part of the interaction, g_s, and Bethe has given arguments to show that it should be accurate as well. On the other hand, (2.1) is only a makeshift approach to the space-exchange part of the interaction. It would be correct if the local-density approximation to the mixed density of neutrons or protons

$$\rho^c(\mathbf{r},\mathbf{r}')=\rho S(\rho,|\mathbf{r}-\mathbf{r}'|),\quad \rho=k_F^3/3\pi^2,\quad S(\rho,t)=3j(2y)/2y,\quad y=k_Ft/2 \quad (2.2)$$

were accurate, because then the contribution to the exchange energy from the interaction of a pair of nucleons would only depend on the density at their center of mass, and would depend on that density in the same way as it would in nuclear matter. This assumption will be criticized below, and an improved treatment of $\rho(\mathbf{r},\mathbf{r}')$ will be offered. This corrected treatment will be shown to be essential for obtaining sensible numerical results. It is important to treat the exchange density well, since, in addition to the antisymmetrization requirement, most of the long-range nucleon-nucleon interaction has a space-exchange character (this is very different from the many-electron problem, where exchange forces are small). It will not be surprising to find in Secs. IV and V that the inhomogeneity corrections to (2.2) are large, because the longest-range part of the nuclear force, the one-pion-exchange diagram, is a space-exchange force.

Variation of (2.1) with respect to ρ leads to the Thomas-Fermi equation,

$$E_F=(\partial/\partial\rho)(\rho(\mathbf{r})W(\rho))+(1+2\kappa)^{-1}U^D(\mathbf{r}), \quad (2.3)$$

[4] W. Kohn and L. J. Sham, Phys. Rev. **137**, A1697 (1965); **140**, A1133 (1965).

[5] P. J. Siemens, Nucl. Phys. **142A**, 225 (1970).

[6] This equation differs from Bethe's because g_D depends on ρ. J. Nemeth and H. A. Bethe [Nucl. Phys. **116A**, 241 (1968)] also use a density-dependent interaction, which they take to depend on the density at the center of mass of the two interacting nucleons, or on the geometric average of the densities at $\mathbf{r}$ and $\mathbf{r}'$. Using the arithmetic average of the densities at $\mathbf{r}$ and $\mathbf{r}'$ is operationally slightly more convenient and should not affect the results. The use of the average density has the advantage that the Thomas-Fermi equation obtained using the c.m. density tends toward instabilities of wavelength about 1 fm, because its kernel is alternating in the relative coordinate; this difficulty does not occur when the average of the endpoint densities is used. It is easy to generalize these equations to different densities of neutrons and protons.

where

$$U^D(\mathbf{r})=\int d^3\mathbf{r}'\{\rho(\mathbf{r}')g_D(\mathbf{r}-\mathbf{r}',\tfrac{1}{2}[\rho(\mathbf{r})+\rho(\mathbf{r}')])$$
$$-\rho(\mathbf{r})g_D(\mathbf{r}-\mathbf{r}',\rho(\mathbf{r}))-\tfrac{1}{2}\rho(\mathbf{r})^2(\partial g_D/\partial\rho)(\mathbf{r}-\mathbf{r}',\rho(\mathbf{r}))$$
$$+\tfrac{1}{2}\rho(\mathbf{r})\rho(\mathbf{r}')(\partial g_D/\partial\rho)(\mathbf{r}-\mathbf{r}',\tfrac{1}{2}[\rho(\mathbf{r})+\rho(\mathbf{r}')])\}. \quad (2.3')$$

The eigenvalue E_F results from the subsidiary condition $\int\rho d^3\mathbf{r}=A$, the total number of nucleons. Bethe[7] has pointed out that if the quantity varied is not W_T but W_T/A, then the eigenvalue in (2.3) must be W_T/A. This condition is necessary since (2.3) can have solutions of a given norm for many values of E_F.

Equation (2.3) as it stands will not have positive solutions of finite norm for most realistic interactions, since W is repulsive at very small densities (because of the kinetic energy required by the exclusion principle). The usual way of overcoming this difficulty is to also permit $\rho=0$ as a solution in most regions of space; this follows trivially from the variation, if, for example, $\rho^{1/2}$ is varied instead of ρ, to ensure that ρ is positive. Bethe[1] has pointed out that a more realistic treatment of the low-density region is to take account of the decaying exponential "tails" of the wave functions at low densities, and to use (2.2) and (2.3) only above a certain density. The difficulty described below does not differ significantly between these two low-density prescriptions.

B. Singular Solutions of Thomas-Fermi Theory

To see that (2.3) has discontinuous solutions, consider the case of a step-function density $\rho=\rho_+$ for $r>R$, $\rho=\rho_-$ for $r<R$, and suppose $\partial g_D/\partial\rho=0$. Then the realizations of (2.3) just inside and outside R are

$$E_F=(\partial/\partial\rho)(\rho W)_{\rho=\rho_+}+(1+2\kappa)^{-1}$$
$$\times\int_{r'<R}d^3\mathbf{r}'(\rho_--\rho_+)g_D(\mathbf{r}-\mathbf{r}'), \quad (2.4a)$$

$$E_F=(\partial/\partial\rho)(\rho W)_{\rho=\rho_-}+(1+2\kappa)^{-1}$$
$$\times\int_{r'>R}d^3\mathbf{r}'(\rho_+-\rho_-)g_D(\mathbf{r}-\mathbf{r}'). \quad (2.4b)$$

The sum and difference of these equations are

$$2E_F\simeq(\partial/\partial\rho)(\rho W)_{\rho=\rho_+}+(\partial/\partial\rho)(\rho W)_{\rho=\rho_-}, \quad (2.5a)$$

$$0=(\partial/\partial\rho)(\rho W)_{\rho_+}-(\partial/\partial\rho)(\rho W)_{\rho_-}$$
$$+(1+2\kappa)^{-1}(\rho_--\rho_+)\int d^3\mathbf{r}'g_D. \quad (2.5b)$$

In (2.5a), the curvature of the surface has been neglected at R, which amounts to supposing that R is much larger than the range of g_D. By a theorem of elementary calculus, (2.5b) can be satisfied when there is a value ρ' between ρ_+ and ρ_- such that

$$(\partial^2/\partial p^2)(\rho W)_{\rho=\rho'}=(1+2\kappa)^{-1}\int d^3\mathbf{r}'g_D(\mathbf{r}'). \quad (2.5c)$$

Equation (2.5c) would be an identity if the nuclear force were an ordinary potential and if W included only the potential energy. However, for realistic g_D and W, condition (2.5c) is not likely to be satisfied, since W includes the potential energy and the saturating parts of the force, as well as the exchange contribution to the energy. For example, the direct force of Ref. 5 gives the right-hand side of (2.5c) a value of about -330 MeV fm^3, which the left-hand side does not reach above one-fifteenth nuclear matter saturation density for the form $W=-24.2\kappa_F^2+11.5\kappa_F^3$ MeV, which has the saturation density and maximum binding energy expected empirically for nuclear matter (this form of W is certainly incorrect at so low a density, especially since it does not begin with a positive coefficient of κ_F^2 as the kinetic energy requires).

However, if ρ_+ is zero, or a specified tail beginning at some density ρ_2 as recommended by Bethe, then (2.4a) does not have to be satisfied. Instead, only (2.4b) remains, which becomes for this case

$$(\partial/\partial\rho)(\rho W)_{\rho=\rho_-}=\tfrac{1}{2}(\rho_--\rho_2)(1+2\kappa)^{-1}\int d^3\mathbf{r}'g_D(\mathbf{r}')+E_F. \quad (2.4c)$$

This condition is easily satisfied; for example, in a real nucleus E_F is expected to be about -8 MeV, and so if g_D and the function W are as mentioned in the last paragraph, then ρ_- will be 0.09 fm^{-3} for $\rho_2=0.03$ fm^{-3}. Clearly, the step density discussed here is an oversimplification, but it ought to be equally clear that discontinuous solutions of (2.3) are to be expected.

A one-dimensional analog of (2.3) was solved on a computer for several curves W and a simplified g_D. g_D was taken as an exponential of range 1.4 fm; its volume integral was varied from -170 to -420 MeV fm^3. The functional form of W was changed, but its saturation density and value at saturation were kept constant. The density was assumed symmetric about $x=0$. This one-dimensional equation corresponds

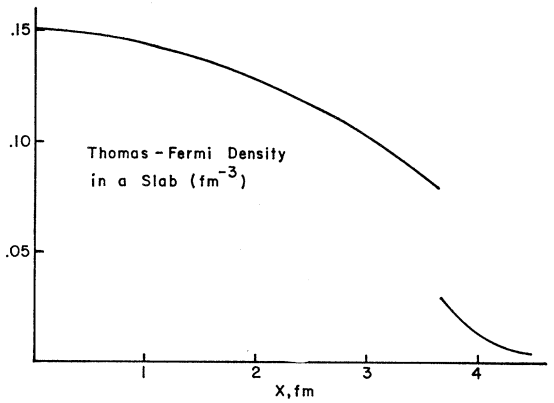

FIG. 1. Discontinuous solution of Thomas-Fermi equation (2.3) for nuclear matter slab, with realistic W and g_D as described in text, Sec. II B.

[7] H. A. Bethe (private communication).

to a three-dimensional slab of nuclear matter $\rho(\mathbf{r})=\rho(x)$, with $g(x)=\int dy\int dz\, g(\mathbf{r})$. Figure 1 shows a typical solution, with W as given above and a strength of g_D which would give -310 MeV fm^3 for the right-hand side of (2.5c). The solution solves (2.3) to better than 0.02 MeV at each of 50 points between $x=0$ and $x=3.6$ fm; at the discontinuity $\rho_-=0.081$ fm^{-3}. This solution has the tail prescribed by Bethe; solutions were also obtained which dropped discontinuously to zero density. The energy per particle E_F was -12.41 MeV for the solution shown, which had 1.16 particles per fm^2 in the slab, including the tails.

C. Reasons for Singular Solutions

Two features of the Thomas-Fermi theory represented by Eq. (2.3) are necessary for the existence of singular solutions. The first is the presence of a zero-range approximation to part of the potential energy. This part of the potential energy is partly a zero-range approximation to the short-range part g_s of the nuclear force—but there is no reason to expect the finite range of g_s to play a critical role in the shape of the nuclear surface—and partly because of the local-density approximation to the exchange energy. The accuracy of the latter approximation will be discussed below in Sec. IV, where the exchange energy is seen to have an important influence on the density distribution.

The other ingredient of the singular solutions of Thomas-Fermi theory is the local-density approximation to the kinetic energy, which amounts to the postulate that the local density is the density of plane-wave states in the local potential $U(\mathbf{r})$, where $U(\mathbf{r})$ is the variational derivative of the total potential energy with respect to the density at point $\mathbf{r}$. This is most easily seen by rewriting Eq. (2.3) as

$$(\hbar^2/2M)k_F(\mathbf{r})^2=E_F-U(\mathbf{r})$$
$$=E_F-(\partial/\partial\rho)[W^*(\rho)\rho(\mathbf{r})]-U^D(\mathbf{r}), \tag{2.3''}$$

where $W^*(\rho)$ is the potential energy per nucleon of uniform nuclear matter at density ρ. Equation (2.3'') is the form in which atomic Thomas-Fermi theory is traditionally presented. From Eq. (2.3''), it is apparent that in Thomas-Fermi theory, the density at a point $\mathbf{r}$ is determined only by the potential at that point, no matter what the potential might be at nearby points. Thus the relation (2.3'') requires the density $\rho(\mathbf{r})=2k_F(\mathbf{r})^3/3\pi^2$ to vary discontinuously if the potential U does. Conversely, the zero-range approximation to part of the nuclear force permits the potential U to vary as rapidly as the density does. There is nothing to prevent discontinuous solutions.

Equation (2.3'') is only expected to be useful when U varies slowly, but its solutions for realistic W^* and g_D vary rapidly. In a rapidly decreasing U, ρ cannot vary as rapidly as (2.3'') prescribes, because the wave functions must anticipate the change in U and begin to decrease before they reach the region in which U varies rapidly. This point is most easily visualized in the case of a square-well potential, where the density will fall off for a distance $1/k_F$ away from the edge of the well. In a nucleus, $1/k_F$ is not much less than the surface thickness, so the effect need not be negligible. Figure 1 demonstrates that it is not.

Thus the variational principle leading from (2.1) to (2.3) is incorrect, because it does not restrict the functions $\rho(\mathbf{r})$ to those which can be generated by physical wave functions. The extrema of (2.1) do not in fact lie among the physically possible functions, but are discontinuous functions; so that the inclusion of unphysical functions in the class of variations is not unimportant, but has the most drastic quantitative effect on the application of the Thomas-Fermi method.

D. Hazardous Extremum of the Chemical Potential

It is perhaps fortunate for the Thomas-Fermi model that it possesses discontinuous solutions, because its continuous solution in a finite nucleus would have an equally objectionable property: It could reach only about two-thirds of nuclear-matter equilibrium density in the interior of the nucleus. This difficulty is associated with the minimum in the chemical potential

$$\mu_{\mathrm{NM}}(\rho)=(\partial/\partial\rho)[\rho W(\rho)], \tag{2.6}$$

which occurs at a density ρ_1 which is about two-thirds of the density ρ_0 at which $W(\rho)$ has its minimum.

Consider the point R in the nuclear surface at which the density goes through ρ_1. The density is a function of the kinetic energy T of the most energetic nucleon,

$$\rho(\mathbf{r})=\rho[T(\mathbf{r})]=\rho[E_F-U(\mathbf{r})].$$

Therefore, the slope of the density is related to the slope of the potential energy,

$$\frac{\partial\rho}{\partial r}=\frac{\partial\rho}{\partial T}\frac{\partial T}{\partial r}=-\frac{\partial\rho}{\partial T}\frac{\partial U}{\partial r}$$
$$=-\frac{\partial\rho}{\partial T}\left(\frac{\partial\mu^*}{\partial r}[\rho(\mathbf{r})]+\frac{\partial}{\partial r}U^D(\mathbf{r})\right), \tag{2.7}$$

where

$$\mu^*(\rho)=(\partial/\partial\rho)[\rho W^*(\rho)] \tag{2.7'}$$

is the potential-energy part of the local nuclear-matter chemical potential. But

$$\frac{\partial\mu^*}{\partial r}(\rho)=\frac{\partial\rho}{\partial r}\frac{\partial\mu^*}{\partial\rho}=\frac{\partial\rho}{\partial r}\frac{\partial}{\partial\rho}(\mu_{\mathrm{NM}}-T)$$
$$=-\frac{\partial\rho}{\partial r}\frac{\partial T}{\partial\rho}\qquad\text{at}\quad r=R, \tag{2.8}$$

since T and ρ are functionally related, while at $\rho(R)=\rho_1$ the chemical potential μ_{NM} has its extremum.

Equations (2.7) and (2.8) together imply that

$$(\partial/\partial r)\,U^D(r)_{r=R}=0$$

at the radius at which the density attains the value ρ_1. With an attractive long-range interaction g_D, U^D has its maximum value at the shoulder where the density begins to drop rapidly. For the experimental density distributions, the maximum of U^D occurs inside the radius at which $\rho=\rho_1$. Worse yet, the repulsive Coulomb potential has a negative slope, so that when it is included, the Thomas-Fermi theory will require $\rho=\rho_1$ not merely at the maximum of U^D, but actually farther inside. Thus in the Thomas-Fermi theory, ρ_1 cannot be attained in the surface, but only inside the nucleus, where the density is a slowly varying function of $\mathbf{r}$. Such a solution is very unsatisfactory: It means that the central density of the nucleus is determined by the surface in such a way that the maximum binding of nuclear matter cannot be exploited.

E. Previous Approximate Solutions and Other Models

Recently,[8] approximate solutions to the Thomas-Fermi equation have been obtained by variation of parameters with certain functional forms. These computations of course have not detected the fact that the solutions are discontinuous.

The integral of g_D appearing in Bethe's theory [Eqs. (2.1) and (2.3)] may be expanded in derivatives of ρ, if the density is not too rapidly varying[1]:

$$\int d^3\mathbf{r}'g_D(\mathbf{r}-\mathbf{r}')[\rho(\mathbf{r}')-\rho(\mathbf{r})]=\tfrac{1}{6}\nabla^2\rho\int d^3\mathbf{r}'g_D(\mathbf{r}')\mathbf{r}'^2. \tag{2.7''}$$

Approximation (2.7'') and a term in $(\nabla\rho)^2$—which is equivalent in (2.1) when integrated by parts—were used by Wilets[3] and by Buchler *et al.*[2] The resulting differential equation naturally has no discontinuous solutions. It might also be claimed that the way in which the differential theory penalizes rapidly varying solutions is reasonable, because the kinetic energy may also be expanded in derivatives of ρ; but the coefficient of this term in the kinetic energy is much smaller than that due to the long-range potential. Besides, such an expansion has been shown by Hohenberg and Kohn[9] to break down near classically forbidden regions. In any case, the differential approximation is not expected to be very reliable, because the thickness of the nuclear surface is comparable to the range of the forces.

Seyler and Blanchard[10] do not obtain discontinuous solutions in their integral theory, because their force has no zero-range components, but relies on a momentum-dependent term to imitate the effects of the exchange force and the saturation of the short-range force. This probably ascribes too long a range to the density dependence of the interaction; and it will be shown below that the treatment of exchange is critical in determining the density distribution. Neither their theory nor the differential theory takes adequate account of the behavior of wave functions near their classically forbidden regions—and Secs. II B and II C have demonstrated the importance of this effect. Thus, these theories cannot be relied on for detailed studies of the shape of the density distribution in the nuclear surface.

[8] I. J. Donnelly, Phys. Letters **28**, 161 (1968).
[9] P. Hohenberg and W. Kohn, Phys. Rev. **136**, B844 (1964).
[10] R. G. Seyler and C. H. Blanchard, Phys. Rev. **131**, 355 (1963).

III. DENSITY AND MIXED DENSITY IN A SEMI-INFINITE POTENTIAL

Kohn and Sham[4] have shown how to calculate densities and other average properties of wave functions near their classical turning points in a one-dimensional potential, using approximate wave functions. In this section their work will be extended to the case of a three-dimensional noninteracting Fermi gas moving in an external potential $U(x)$ which is a function of only one of the three Cartesian coordinates. The results of this analysis will be applied to the nuclear surface in Sec. IV.

Consider a three-dimensional gas of noninteracting spin-$\frac{1}{2}$ particles moving nonrelativistically in a potential $U(x)$ which approaches a constant value U_0 for large negative x, and which increases monotonically with x. When convenient it will be assumed that the particles are in a large box, though the results will be taken in the limit of infinite volume. The ground state of the system may be characterized by a Fermi energy E_F separating occupied and unoccupied single-particle states. The one-particle Schrödinger equation is

$$(H_x-E_x+H_y-E_y+H_z-E_z)\Psi=0, \tag{3.1a}$$

$$H_x-E_x=V(x)-\partial^2/\partial x^2-k_x^2-V_0,$$

$$H_y-E_y=-\partial^2/\partial y^2-k_y^2, \tag{3.1b}$$

$$H_z-E_z=-\partial^2/\partial z^2-k_z^2,$$

where $V(x)=2MU(x)/\hbar^2$ is the reduced potential. Equation (3.1) may be separated by factoring Ψ,

$$H_x\psi_x=E_x\psi_x, \tag{3.2a}$$

$$H_y\psi_y=E_y\psi_y, \tag{3.2b}$$

$$H_z\psi_z=E_z\psi_z, \tag{3.2c}$$

$$\Psi(x,y,z)=\psi_x(x)\psi_y(y)\psi_z(z). \tag{3.2d}$$

The solutions ψ_y and ψ_z are plane waves while the solutions ψ_x depend on $V(x)$. The Green's function for Eq. (2.2a) may be written as

$$G_x(x,x',E)=\sum_m \psi_x(x,E_m)\psi_x(x',E_m)/(E-E_m), \tag{3.3}$$

where the index m denotes the eigenstates of (3.2a).

It is important to notice that G_x is *not* the Green's function of the three-dimensional problem (3.1a), but only of the one-dimensional Schrödinger equation. The advantage of using G_x rather than a three-dimensional Green's function is that Kohn and Sham[4] have developed techniques for calculating G_x which are not easily generalized to the three-dimensional Green's function.

The Dirac mixed density $\rho(\mathbf{r}, \mathbf{r}')$ may be expressed in terms of the Green's function G_x. For by its definition,

$$\rho(\mathbf{r}, \mathbf{r}') = \sum_{m_x}\sum_{m_y}\sum_{m_z} \psi_x^*(x, E_{m_x})\psi_y^*(y, E_{m_y})\psi_z^*(z, E_{m_z}) \times\psi_x(x', E_{m_x})\psi_y(y', E_{m_y})\psi_z(z', E_{m_z}) \quad (3.4a)$$

$$= 2\int[d^3k/(2\pi)^3]\psi_x^*(x, k_x^2)\psi_x(x', k_x^2) \times e^{-ik_y(y-y')}e^{-ik_z(z-z')}, \quad (3.4b)$$

where E_F is also expressed in reduced units. (3.4b) follows from (3.4a) because the spectrum of H is determined by the region of constant potential to the left. The integrals over k_z and k_y lead to

$$\rho(\mathbf{r}, \mathbf{r}') = (2\pi^2)^{-1}\int_0^{k_F} dk_x(k_F^2-k_x^2)J[r_\perp(k_F^2-k_x^2)^{1/2}] \times\psi_x^*(x, k_x^2)\psi_x(x', k_x^2)$$

$$= (2\pi)^{-1}\sum_{|k_x|<k_F}(E_F-E_x)J[r_\perp(E_F-F_x)^{1/2}] \times\psi_x^*(x, E_x)\psi_x(x', E_x), \quad (3.5)$$

where $r_\perp^2=(y-y')^2+(z-z')^2$ and $J(t)=2J_1(t)/t$. The limits on all the sums and integrals are over occupied states, so that $k_F^2=2M(E_F-U_0)/\hbar^2$. It follows immediately from (3.5) and (3.3) that the relation between $\rho(\mathbf{r}, \mathbf{r}')$ and G_x is

$$\rho(\mathbf{r}, \mathbf{r}') = (4\pi^2 i)^{-1}\oint_C dE \times(E_F-E)G_x(x, x', E)J[r_\perp(E_F-E)^{1/2}], \quad (3.6)$$

where the contour C encloses the real axis up to E_F (Fig. 2).

As an example, for WKB wave functions in a slowly varying potential far from their classical turning points, Kohn and Sham have shown that

$$G_x(x, x', E) = (1/2i)[p(x, E)p(x', E)]^{-1/2} \times\exp[\pm i\theta(x, x', E)] \quad \text{for} \quad x\gtrless x', \quad (3.7)$$

where

$$p(x, E) = [E-V(x)]^{1/2},$$
$$\theta(x, x', E) = \int_x^x dtp(t, E), \quad (3.8)$$

and there is a branch cut extending to $+\infty$ from the minimum value of V in the interval (x, x'). If the potential is constant $V(x)=V_0$, then the integrals are straightforward and (2.2) is obtained.

To learn about the behavior of the density in the region of classical turning points, it is useful to calculate $\rho(\mathbf{r}, \mathbf{r}')$ for a ramp potential $V(x)=(x-\alpha_F)V'+E_F$, where α_F is the classical turning point of a particle of energy E_F. The Green's function found by Kohn and Sham for $x>x'$ and $\mathrm{Im}E>0$ is

$$G_x(x, x', E) = \frac{\pi}{3i}\left(\frac{\theta(x, E)\theta(x', E)}{p(x, E)p(x', E)}\right)^{1/2}\{J_{1/3}[\theta(x, E)] + J_{-1/3}[\theta(x', E)]\}\{e^{i\pi/3}J_{1/3}[\theta(x, E)] + e^{-i\pi/3}J_{-1/3}[\theta(x', E)]\}, \quad (3.9)$$

where $\theta(x, E)=\theta(\alpha_E, x, E)$, and α_E is the classical turning point for energy E, i.e., $V(\alpha_E)=E$. Using (3.9) in Eq. (3.6) for the mixed density, noting that $G_x(E-i\epsilon)=G_x^*(E+i\epsilon)$, and changing variables to $z=(V')^{-2/3}\{E-\frac{1}{2}[V(x)+V(x')]\}$ leads to

$$\rho(\mathbf{r}, \mathbf{r}') = \tfrac{1}{2}V'\int_{-\infty}^{z_F} dz(z_F-z)J[2s(z_F-z)^{1/2}] \times\mathrm{Ai}(-z+\zeta)\mathrm{Ai}(-z-\zeta), \quad (3.10)$$

where

$$z_F=(V')^{-2/3}\{E_F-\tfrac{1}{2}[V(x)+V(x')]\},$$
$$s=\tfrac{1}{2}r_\perp(V')^{1/3},$$
$$\zeta=(V')^{1/3}(x-x')/2,$$

and Ai represents the ordinary Airy function of the first kind.[11]

To obtain an explicit expression for $\rho(\mathbf{r}, \mathbf{r}')$, the Bessel and Airy functions of Eqs. (3.10) may be expanded in powers of $s(z_F-z)^{1/2}$ and ζ, respectively,

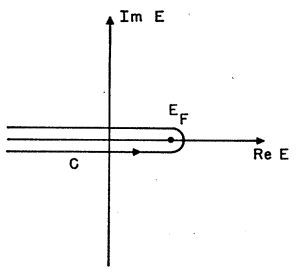

FIG. 2. Contour C used in evaluating Eq. (3.6).

TABLE I. First few Airy-function derivatives appearing in Eq. (3.12) of the text.

k	$(\partial/\partial\zeta)^{2k}[\mathrm{Ai}(-z+\zeta)\mathrm{Ai}(-z-\zeta)]$ at $\zeta=0$
0	$\mathrm{Ai}(-z)^2$
1	$-2[z\mathrm{Ai}(-z)^2+\mathrm{Ai}'(-z)^2]$
2	$4[2z^2\mathrm{Ai}(-z)^2+2z\mathrm{Ai}'(-z)^2-\mathrm{Ai}(-z)\mathrm{Ai}'(-z)]$

[11] In terms of Bessel functions, $3z^{-1/2}\mathrm{Ai}(-z)=[J_{1/3}(t)+J_{-1/3}(t)]$, where $3t=2z^{3/2}$.

giving

$$\rho(\mathbf{r},\mathbf{r}')=(2\pi)^{-1}V'\sum_k\sum_l \zeta^{2k}s^{2l}(z_F)^{k+l}I_{kl}(z_F), \quad (3.11)$$

where

$$I_{kl}(z_F)=[l!(l+1)!]^{-1}\int_{-\infty}^{z_F}\frac{dz}{z_F^2}(z_F-z)^{l+1}\frac{(-1)^l}{(2k)!}$$
$$\times\left(\frac{\partial}{\partial\zeta}\right)^{2k}[\mathrm{Ai}(-z-\zeta)\ \mathrm{Ai}(-z+\zeta)]_{\zeta=0}. \quad (3.12)$$

Table I shows the first few derivatives needed for evaluating Eq. (3.12), which may be obtained by means of the differential equation $\mathrm{Ai}''(z)=z\,\mathrm{Ai}(z)$. Very likely a closed-form expression for I_{kl} can be found, but this has not been done. Instead, the first few of the I_{kl} have been evaluated, making use of the integrals

$$\begin{aligned}
&\int dy\,\mathrm{Ai}(-y)^2=y\,\mathrm{Ai}(-y)^2+\mathrm{Ai}'(-y)^2,\\
&3\int dy\,\mathrm{Ai}(-y)^2y=y^2\,\mathrm{Ai}(-y)^2+y\,\mathrm{Ai}'(-y)^2\\
&\qquad+\mathrm{Ai}(-y)\ \mathrm{Ai}'(-y),\\
&5\int dy\,\mathrm{Ai}(-y)^2y^2=(y^3+1)\ \mathrm{Ai}(-y)^2+y^2\,\mathrm{Ai}'(-y)^2\\
&\qquad+2y\,\mathrm{Ai}(-y)\ \mathrm{Ai}'(-y),\\
&7\int dy\,\mathrm{Ai}(-y)^2y^3=y^4\,\mathrm{Ai}(-y)^2+(y^3-3)\ \mathrm{Ai}'(-y)^2\\
&\qquad+3y^2\,\mathrm{Ai}(-y)\ \mathrm{Ai}'(-y), \quad (3.13)\\
&3\int dy\,\mathrm{Ai}'(-y)^2=y^2\,\mathrm{Ai}(-y)^2+y\,\mathrm{Ai}'(-y)^2\\
&\qquad-2\,\mathrm{Ai}(-y)\ \mathrm{Ai}'(-y),\\
&5\int dy\,\mathrm{Ai}'(-y)^2y=(y^3-\tfrac{3}{2})\ \mathrm{Ai}(-y)^2+y^2\,\mathrm{Ai}'(-y)^2\\
&\qquad-3y\,\mathrm{Ai}(-y)\ \mathrm{Ai}'(-y),\\
&7\int dy\,\mathrm{Ai}'(-y)^2y^2=y^4\,\mathrm{Ai}(-y)^2+(y^3+4)\ \mathrm{Ai}'(-y)^2\\
&\qquad-4y^2\,\mathrm{Ai}(-y)\ \mathrm{Ai}'(-y),
\end{aligned}$$

which may be verified by differentiation. The resulting expression for the mixed density is

$$\begin{aligned}
\rho(\mathbf{r},\mathbf{r}')=(1/2\pi)\,V'\{&\tfrac{2}{3}[z_F^2\,\mathrm{Ai}(-z_F)^2+z_F\,\mathrm{Ai}'(-z_F)^2\\
&-\tfrac{1}{2}\,\mathrm{Ai}(-z_F)\ \mathrm{Ai}'(-z_F)][1-\tfrac{2}{5}(\zeta^2+s^2)z_F\\
&+(2/35)(\zeta^2+s^2)^2z_F^2]-\tfrac{1}{10}\mathrm{Ai}(-z_F)^2(\zeta^2+s^2)\\
&+\tfrac{1}{20}(\zeta^2+s^2)^2[z_F\,\mathrm{Ai}(-z_F)^2+\tfrac{5}{7}\,\mathrm{Ai}'(-z_F)^2]\} \quad (3.14)
\end{aligned}$$

plus terms of order $|\mathbf{r}-\mathbf{r}'|^6$. It is remarkable that, to this order, the mixed density is isotropic in the relative coordinate $(\mathbf{r}-\mathbf{r}')$, as first noted by Lin.[12]

It is instructive to recast Eq. (3.14) in a form in which V' does not appear explicitly. This may be done for $\frac{1}{2}(x+x')<\alpha_F$ by using for z_F the equivalent definition

$$z_F=[\tfrac{3}{2}\theta(\tfrac{1}{2}(x+x'),E_F)]^{2/3}$$
$$=\left\{\frac{3}{2}\int_{(x+x')/2}^{\alpha_F}dt[E_F-V(t)]^{1/2}\right\}^{2/3}, \quad (3.15)$$

[12] Y. C. Lin, thesis, Cornell University, 1969 (unpublished).

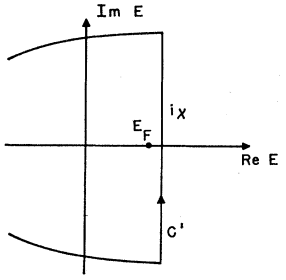

FIG. 3. Contour C' used in evaluating Eq. (3.19).

and by defining

$$k_F=\{E_F-V[\tfrac{1}{2}(x+x')]\}^{1/2}; \quad (3.16)$$

when $\frac{1}{2}(x+x')>\alpha_F$, the appropriate definitions are

$$z_F=-\left\{-\frac{3}{2}\int_{(x+x')/2}^{\alpha_F}dt[V(t)-E_F]^{1/2}\right\}^{2/3} \quad (3.15')$$

and

$$k_F=i\{V[\tfrac{1}{2}(x+x')]-E_F\}^{1/3}$$
$$=i\gamma_F. \quad (3.16')$$

Then the mixed density is given by

$$\begin{aligned}
\rho(\mathbf{r},\mathbf{r}')=(k_F^3/3\pi^2)\{&\pi(1-\tfrac{2}{5}y^2+\tfrac{2}{35}y^4)\\
&\times[z_F^{1/2}\,\mathrm{Ai}(-z_F)^2+z_F^{-1/2}\,\mathrm{Ai}'(-z_F)^2\\
&-\tfrac{1}{2}z_F^{-3/2}\,\mathrm{Ai}(-z_F)\ \mathrm{Ai}'(-z_F)]\\
&-\tfrac{3}{2}\pi z_F^{-3}[\tfrac{1}{10}y^2z_F^{1/2}\,\mathrm{Ai}(-z_F)^2-\tfrac{1}{20}(y^4z_F^{1/2}\,\mathrm{Ai}(-z_F)^2\\
&+\tfrac{5}{7}z_F^{-1/2}\,\mathrm{Ai}'(-z_F)^2)]\}, \quad (3.17)
\end{aligned}$$

where $y=|\mathbf{r}-\mathbf{r}'|\,k_F/2$.

For large z_F, asymptotic forms of the Airy functions lead to the expression

$$\begin{aligned}
\rho(\mathbf{r},\mathbf{r}')=(k_F^3/3\pi^2)\{&[1-\tfrac{1}{12}\theta_F^{-2}(\tfrac{5}{4}\tfrac{2}{3}\tfrac{7}{2}+\tfrac{2}{4}\tfrac{3}{3}\tfrac{3}{2}\sin2\theta_F)]\\
&\times(1-\tfrac{2}{5}y^2+\tfrac{2}{35}y^4)+\tfrac{1}{12}\theta_F^{-2}[-\tfrac{2}{5}y^2(1+\sin2\theta_F)\\
&+\tfrac{1}{2}\tfrac{2}{5}y^4(1+\tfrac{1}{6}\sin2\theta_F)]\}, \quad (3.18)
\end{aligned}$$

as $x\to-\infty$, where

$$\theta_F=\int_{(x+x')/2}^{\alpha_F}dt[E_F-V(t)]^{1/2}.$$

Thus the mixed density approaches the local-density approximation (2.2) with θ_F^{-2} away from the classical turning point α_F; and the coefficient of θ_F^{-2} is small. This rapid approach is to be contrasted with the one-dimensional Fermi gas studied by Kohn and Sham, in which the density approaches the classical density only as θ_F^{-1}. The reason may be seen by examining Eqs. (3.6). Following Kohn and Sham, a change of variables $E=E_F+i\chi$ and a deformation of the contour of integration to that of Fig. 3 show that

$$\rho(\mathbf{r},\mathbf{r}')-\rho^c(\mathbf{r},\mathbf{r}')\times=-(2\pi)^{-1}\,\mathrm{Im}\int_0^\infty\chi d\chi$$
$$\times J[r_\perp(E_F+i\chi)^{1/2}][G_x(E_F+i\chi)-G_x^c(E_F+i\chi)], \quad (3.19)$$

where ρ^c is the local-density approximation given in

(2.2). Kohn and Sham, who obtain a similar expression involving the real part and without the factor χ, argue that the main contribution to the difference from the local-density approximation is from the region $\chi \simeq 0$ near the Fermi energy E_F—that is, from the waves near the top of the Fermi sea. However, the extra factor (E_F-E) in Eq. (3.6), or χ in (3.19), suppresses this contribution, so that the difference appears only in higher order. The suppression is directly due to the fact that in a three-dimensional (as contrasted with a one-dimensional) Fermi gas, there are few states with k_x near k_F. As a result of this suppression, the oscillations of density noted by Kohn and Sham occur only very near the classical turning point of the most energetic particle. This feature ought also to be found in a statistical treatment of electron densities in atoms.

IV. APPLICATION TO NUCLEAR SURFACE

A. Single-Particle Potential

Because the mixed density for the ramp potential can be expressed in a way [Eq. (3.17)] that does not explicitly use the form of the potential, and because this expression very rapidly approaches the constant-potential expression away from the classical turning point of the last nucleon [Eq. (3.18)] it is tempting to use the expression (3.17) to relate the nuclear density to the potential felt by nucleons in a real nucleus. For the ordinary density $\rho(\mathbf{R}, \mathbf{R})$, where $\mathbf{R}=\frac{1}{2}(\mathbf{r}+\mathbf{r}')$, this may be done by using (3.17) even though the potential is not a linear one. For the mixed density, however, since the corrections to the local-density expression have only been computed to second order in y^2 (i.e., fourth order in the relative distance), some estimate of the remaining terms must be made. Inspecting Eq. (3.17) and (3.18) suggests the form

$$\rho(\mathbf{r}, \mathbf{r}') = \rho(\mathbf{R}, \mathbf{R}) S(\rho(\mathbf{R}, \mathbf{R}); |\mathbf{r}-\mathbf{r}'|) f(y^2, z_F) \quad (4.1)$$

for $R<\alpha_F$. The function S in (4.1) is the local-density ratio of mixed and ordinary density [cf. Eq. (2.2)];

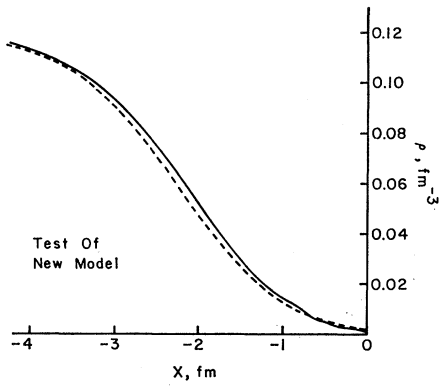

FIG. 4. Comparison of approximate (solid curve) and exact (dashed curve) densities in an analytic potential (text, Sec. IV A). Exact curve courtesy Y. C. Lin.

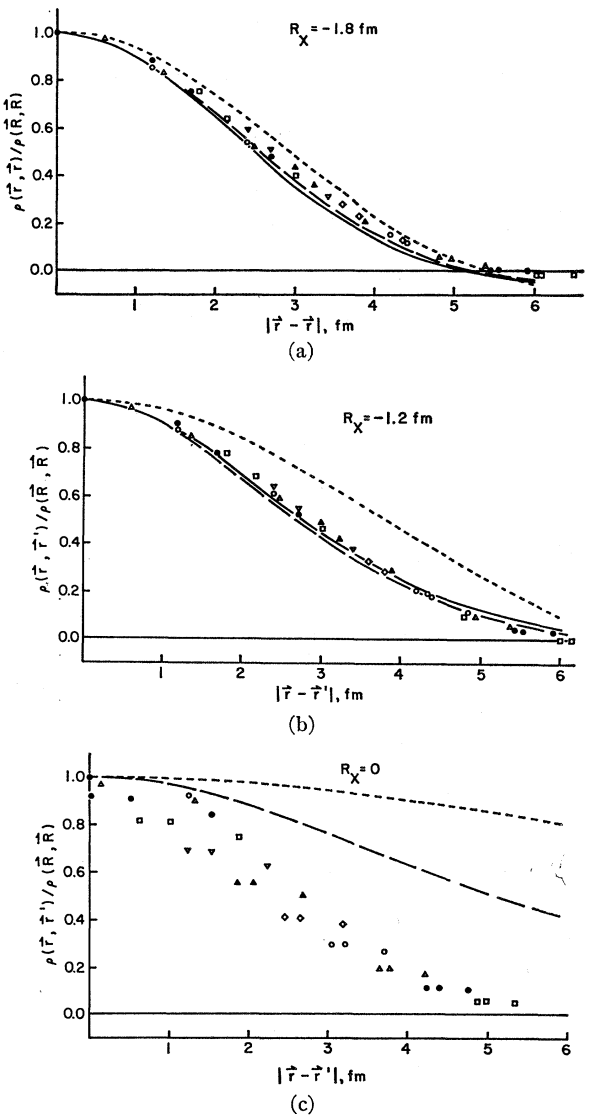

FIG. 5. Comparison of approximation (4.1) (solid curve) and exact calculation (individual points with several symbols) for the mixed density in an analytic potential. The various symbols for the exact mixed density distinguish different values of $r_\perp$. Curve with short dashes is for $f=1$ in Eq. (4.1). Curve with long dashes is for the additional approximation (4.2). Exact values from Y. C. Lin.

its use is suggested by the appearance of the first three terms of its power-series expansion in (3.17). The function $f(y^2, z_F)$ is to be guessed from its first three terms in y^2, which have been calculated. The second and third terms seem of about equal magnitude and alternate in sign; thus a geometric series is hazarded for f:

$$1/f(y^2, z_F) \simeq 1+(3y^2/20) z_F^{-3}[z_F^{1/2}\,\mathrm{Ai}(-z_F)^2] \times [z_F^{1/2}\,\mathrm{Ai}(-z_F)^2 + z_F^{-1/2}\,\mathrm{Ai}'(-z_F)^2 - z_F^{-3/2}\,\mathrm{Ai}(-z_F)\,\mathrm{Ai}'(-z_F)]^{-1}. \quad (4.1')$$

The accuracy of using (3.17) for ρ even in the

interior of the nucleus, and the usefulness of the extrapolation (4.1), have been tested by comparing their numerical predictions with the computer calculations of wave functions in a potential done by Lin, and reported in his thesis at Cornell[12] as well as in Bethe's paper.[1] Lin used a potential $U(x)=-40\,\mathrm{MeV}(1-e^{x/a})^2$, with $a=1.2$ fm, filled to $E_F=-8$ MeV (the sign of x used here is the reverse of Lin's notation); he set $U(x)=0$ for $x>0$. A comparison of his results with those of the present theory are shown in Figs. 4 and 5. According to this test, the theory developed here may be relied on for finding $\rho(\mathbf{r},\mathbf{r}')$ at least to the classical turning point of the most energetic nucleon (-0.7 fm in this example). The new approximation is more accurate than the relation between mixed and ordinary densities of the classical (Slater) approximation, viz., $f=1$ and k_F determined by the local density, which is also shown in Fig. 5.

In order to obtain a useful expression for the single-particle potential, it is desirable to make the exchange energy, as far as possible, a function of the local density, as it is in the Thomas-Fermi model of Bethe. The form (4.1) for the exchange density may be further modified to eliminate the potential from the definition (2.2) of y, taking instead

$$y\simeq\tfrac{1}{2}(3\pi^2\rho)^{1/3}\,|\,\mathbf{r}-\mathbf{r}'\,|\,. \tag{4.2}$$

Then $\rho(\mathbf{r},\mathbf{r}')$ may be expressed in terms of the local density $\rho(\mathbf{R},\mathbf{R})$, except for the dependence of f on z_F. This redefinition does not reduce the accuracy of (4.1), as is shown by Fig. 5, which also compares the approximation (4.2) to Lin's results in the test case described above.

Thus, it is still possible to write the total nuclear potential energy W_T^* as a sum of a local-density expression plus long-range corrections. Define

$$F(\rho,|\,\mathbf{r}-\mathbf{r}'\,|,z_F)=f(y^2,z_F), \tag{4.3}$$

and let $g^u(r,\rho)$ be the nuclear effective force between unlike particles, $g^l(r,\rho)$ between like particles; g_D is the direct force and $g\chi$ is the space-exchange force.[13] Then [introducing different neutron and proton densities $N(\mathbf{r})$ and $P(\mathbf{r})$, and their corresponding wave-number integrals z_n and z_p], the total potential energy of the nucleus is

$$W_T^*=\int d^3\mathbf{r}\rho(\mathbf{r})W^*(N(\mathbf{r}),P(\mathbf{r}))+(1+2\kappa)^{-1}(W_D+W_\chi)+\text{coulomb}, \tag{4.4}$$

where $W^*(\rho)$ is the potential energy per nucleon of uniform nuclear matter, and W_D and W_χ are the inhomogeneity corrections to W_T^*:

$$\begin{aligned}W_D=\frac{1}{2}\int d^3\mathbf{r}\int d^3\mathbf{r}'\Big\{&N(\mathbf{r})\Big[N(\mathbf{r}')g_D{}^l\Big(\mathbf{r}-\mathbf{r}',\frac{N(\mathbf{r})+N(\mathbf{r}')}{2}\Big)-N(\mathbf{r})g_D{}^l(\mathbf{r}-\mathbf{r}',N(\mathbf{r}))\Big]\\&+P(\mathbf{r})\Big[P(\mathbf{r}')g_D{}^l\Big(\mathbf{r}-\mathbf{r}',\frac{P(\mathbf{r})+P(\mathbf{r}')}{2}\Big)-P(\mathbf{r})g_D{}^l(\mathbf{r}-\mathbf{r}',P(\mathbf{r}))\Big]\\&+2P(\mathbf{r})\Big[N(\mathbf{r}')g_D{}^u\Big(\mathbf{r}-\mathbf{r}',\frac{P(\mathbf{r})+N(\mathbf{r}')}{2}\Big)-N(\mathbf{r})g_D{}^u\Big(\mathbf{r}-\mathbf{r}',\frac{P(\mathbf{r})+N(\mathbf{r})}{2}\Big)\Big]\Big\}\end{aligned} \tag{4.5}$$

and

$$\begin{aligned}W_X=-\tfrac{1}{2}\int d^3\mathbf{R}\int d^3\mathbf{r}\{&N(\mathbf{R})^2S(N(\mathbf{R}),r)^2g_X{}^l(r,N(\mathbf{R}))[1-F(N(\mathbf{R}),r,z_n(\mathbf{R}))^2]\\&+P(\mathbf{R})^2S(P(\mathbf{R}),r)^2g_X{}^l(r,P(\mathbf{R}))[1-F(P(\mathbf{R}),r,z_p(\mathbf{R}))^2]\\&+2N(\mathbf{R})P(\mathbf{R})S(N(\mathbf{R}),r)S(P(\mathbf{R}),r)g_X{}^u(r,[N(\mathbf{R})+P(\mathbf{R})]/2)\\&\times[1-F(N(\mathbf{R}),r,z_n(\mathbf{R}))F(P(\mathbf{R}),r,z_p(\mathbf{R}))]\}.\end{aligned} \tag{4.6}$$

The correlations between nucleons are taken into account by means of the density-dependent interaction $g(r,\rho)$, as has been explained in Ref. 5.

The manipulation leading to (4.4)–(4.6) is crucial to the formulation of a simple statistical theory of the nucleus, because it is only when the total potential energy may be written as a functional of the local density, that there is a local wave equation for the single-particle wave functions Ψ. If the exchange density cannot be simplified, then the variational problem of minimizing the total energy with respect to the wave functions leads to a nonlocal wave equation of the Hartree-Fock type,

$$E\Psi(\mathbf{r})=-(\hbar^2/2M)\nabla^2\Psi(\mathbf{r})+\Psi(\mathbf{r})\int d^3\mathbf{r}'\rho(\mathbf{r}')g_D(\mathbf{r}-\mathbf{r}')+\int d^3\mathbf{r}'\rho(\mathbf{r},\mathbf{r}')g_X(\mathbf{r}-\mathbf{r}')\Psi(\mathbf{r}')+\text{derivatives of } g(\rho).$$

But when the exchange energy has been written in terms

[13] In terms of the spin-parity components of the nuclear force described in Ref. 5, the direct and exchange forces for like and unlike nucleons are $g_D{}^l=(g_{se}+3g_{to})/4$, $g_X{}^l=(g_{se}-3g_{to})/4$; $g_D{}^u=(g_{se}+3g_{te}+g_{so}+3g_{to})/8$, $g_X{}^u=(g_{se}+3g_{te}-g_{so}-3g_{to})/8$, where s means spin singlet, t means spin triplet, e means even L, and o means odd L. The use of direct and exchange forces defined in this way takes account of the antisymmetrization of the wave functions, as well as the space-exchange nature of the force.

of only the local density $\rho(\mathbf{r})$, then the variation of that expression leads to a Hartree-type local wave equation

$$E\Psi(\mathbf{r}) = -(\hbar^2/2M)\nabla^2\Psi(\mathbf{r}) + \Psi(\mathbf{r})[\delta/\delta\rho(r)]W_T^*[\rho].$$

Such a local wave equation has been assumed in the formal development of Sec. III.

The expression obtained above for W_T^* is not quite entirely dependent on the local density. It also depends on the wave-number integrals z_n and z_p. Their values affect the contributions to the energy from the region close to the classical turning point of the most energetic particle, as was shown in Eq. (3.18). The dependence of z_n and z_p on the density distribution would contribute a correction to the inhomogeneity correction to the single-particle potential [Eq. (4.9)]. Because the integrals defining z_n and z_p range only over the region from the point at which the mixed density is being computed, to the classical turning point of the most energetic nucleon, almost all the additional contribution to the single-particle potential will be localized in the region very near α_F. In this region of very low densities, the nuclear-matter potential energy $W^*(\rho)$ is not very well known either, so it seems unjustifiable to include the very complicated variation of W_T^* with respect to z_n and z_p in computing the single-particle potential.

If that variation is ignored, then the potential seen by a neutron or proton is found by taking the variation of W_T^* with respect to its explicit dependence on $N(\mathbf{r})$ or $P(\mathbf{r})$. The result for the neutron single-particle potential is

$$U_n(\mathbf{r}) = [\partial/\partial N(\mathbf{r})]\{[N(\mathbf{r})+P(\mathbf{r})]W^*(N(\mathbf{r}), P(\mathbf{r}))\} + (1+2\kappa)^{-1}[U_n{}^D(\mathbf{r}) + U_n{}^X(\mathbf{r})], \quad (4.7)$$

where $U_n{}^D$ and $U_n{}^X$ represent the inhomogeneity corrections arising from the direct and exchange potentials, respectively:

$$U_n{}^D(\mathbf{r}) = \int d^3\mathbf{r}' \Big\{ N(\mathbf{r}')g_D{}^l\Big(\mathbf{r}-\mathbf{r}', \frac{N(\mathbf{r})+N(\mathbf{r}')}{2}\Big) + P(\mathbf{r}')g_D{}^u\Big(\mathbf{r}-\mathbf{r}', \frac{P(\mathbf{r}')+N(\mathbf{r})}{2}\Big) - N(\mathbf{r})g_D{}^l(\mathbf{r}-\mathbf{r}', N(\mathbf{r})) - P(\mathbf{r})g_D{}^u\Big(\mathbf{r}-\mathbf{r}', \frac{P(\mathbf{r})+N(\mathbf{r})}{2}\Big) + \tfrac{1}{2}N(\mathbf{r})\Big[N(\mathbf{r}')h_D{}^l\Big(\mathbf{r}-\mathbf{r}', \frac{N(\mathbf{r})+N(\mathbf{r}')}{2}\Big) + P(\mathbf{r}')h_D{}^u\Big(\mathbf{r}-\mathbf{r}', \frac{P(\mathbf{r}')+N(\mathbf{r})}{2}\Big) - N(\mathbf{r})h_D{}^l(\mathbf{r}-\mathbf{r}', N(\mathbf{r})) - P(\mathbf{r})h_D{}^u\Big(\mathbf{r}-\mathbf{r}', \frac{P(\mathbf{r})+N(\mathbf{r})}{2}\Big)\Big]\Big\}, \quad (4.8)$$

$$\begin{aligned} U_n{}^X(\mathbf{r}) = -\int d^3\mathbf{r}' \Big\{ & N(\mathbf{r})S(N(\mathbf{r}), \mathbf{r}')^2 g_X{}^l(\mathbf{r}', N(\mathbf{r}))[1-F(N(\mathbf{r}), \mathbf{r}', z_n(\mathbf{r}))^2] \\ & + P(\mathbf{r})S(P(\mathbf{r}), \mathbf{r}')S(N(\mathbf{r}), \mathbf{r}')g_X{}^u\Big(\mathbf{r}', \frac{P(\mathbf{r})+N(\mathbf{r})}{2}\Big)[1-F(P(\mathbf{r}), \mathbf{r}', z_p(\mathbf{r}))F(N(\mathbf{r}), \mathbf{r}', z_n(\mathbf{r}))] \\ & + N(\mathbf{r})^2 S'(N(\mathbf{r}), \mathbf{r}')S(N(\mathbf{r}), \mathbf{r}')g_X{}^l(\mathbf{r}', N(\mathbf{r}))[1-F(N(\mathbf{r}), \mathbf{r}', z_n(\mathbf{r}))^2] \\ & + P(\mathbf{r})N(\mathbf{r})S'(N(\mathbf{r}), \mathbf{r}')S(P(\mathbf{r}), \mathbf{r}')g_X{}^u\Big(\mathbf{r}', \frac{P(\mathbf{r})+N(\mathbf{r})}{2}\Big)[1-F(P(\mathbf{r}), \mathbf{r}', z_p(\mathbf{r}))F(N(\mathbf{r}), \mathbf{r}', z_n(\mathbf{r}))] \\ & + \tfrac{1}{2}N(\mathbf{r})^2 S(N(\mathbf{r}), \mathbf{r}')^2 h_X{}^l(\mathbf{r}', N(\mathbf{r}))[1-F(N(\mathbf{r}), \mathbf{r}', z_n(\mathbf{r}))^2] + \tfrac{1}{2}P(\mathbf{r})N(\mathbf{r})S(P(\mathbf{r}), \mathbf{r}')S(N(\mathbf{r}), \mathbf{r}') \\ & \times h_X{}^u\Big(\mathbf{r}', \frac{P(\mathbf{r})+N(\mathbf{r})}{2}\Big)[1-F(P(\mathbf{r}), \mathbf{r}', z_p(\mathbf{r}))F(N(\mathbf{r}), \mathbf{r}', z_n(\mathbf{r}))] - N(\mathbf{r})^2 S(N(\mathbf{r}), \mathbf{r}')^2 g_X{}^l(\mathbf{r}, N(\mathbf{r})) \\ & \times F'(N(\mathbf{r}), \mathbf{r}', z_n(\mathbf{r}))F(N(\mathbf{r}), \mathbf{r}', z_n(\mathbf{r})) - P(\mathbf{r})N(\mathbf{r})S(P(\mathbf{r}), \mathbf{r}')S(N(\mathbf{r}), \mathbf{r}')g_X{}^u\Big(\mathbf{r}', \frac{P(\mathbf{r})+N(\mathbf{r})}{2}\Big) \\ & \times F'(N(\mathbf{r}), \mathbf{r}', z_n(\mathbf{r}))F(P(\mathbf{r}), \mathbf{r}', z_p(\mathbf{r}))\Big\}. \end{aligned} \quad (4.9)$$

Here $h(r, \rho)$, $F'(\rho, r, z)$, and $S'(\rho, r)$ are the derivatives with respect to density of $g(r, \rho)$, $F(\rho, r, z)$, and $S(\rho, r)$, respectively. The prescriptions of Ref. 5 have been followed for the density dependence of the neutron-proton force. Similar expressions may be obtained for the proton potential.

The new statistical model of the nucleus is seen to consist of two sets of equations: (3.17) and (4.1)–(4.3) to find the density and mixed density in a potential $U(\mathbf{r})$, and (4.7)–(4.9) to calculate the potential due to a given density and mixed density. The relations for finding the density from the potential

should be corrected for the fact that the nuclear surface is spherical rather than planar.[14] This correction has not been made in the present work. On the other hand, the spherical geometry is easily handled correctly in the step of finding the potential due to a particular density and mixed density. To learn the numerical predictions of the statistical model for a given nuclear-matter energy surface $W^*(N, P)$ and long-range density-dependent interaction g, it is necessary to iterate the steps

$$\text{potential}\rightarrow\text{density}\rightarrow\text{potential}$$

until self-consistency is achieved. The eigenvalues E_n and E_p, the neutron and proton Fermi energies, are to be determined in the step potential→density by the condition that the resulting distributions of neutrons and protons have the desired norms.

B. Region of Very Low Density

In the region beyond the classical turning point of the most energetic nucleon, the classical density and mixed density vanish. Thus there is no quasiclassical motivation for the form (4.1), which, in fact, cannot be applied since k_F is imaginary, and though it would still be possible to use (4.2), that form does not prove very accurate beyond the last classical turning point [Fig. 5(c)]. On the other hand, the correction to the exchange potential in this part of the surface is too large to ignore. Lin's result [Fig. 5(c)] suggests that beyond the classical turning point α_F it might be acceptable to use the same dependence of $\rho(\mathbf{r}, \mathbf{r}')$ on $|\mathbf{r}-\mathbf{r}'|$ as it has at α_F. This has been done in the numerical work reported below; it should be emphasized that it is purely an *ad hoc* procedure. On the other hand, because of the treatment of this low-density region (see next paragraphs), almost none of the numerical results are affected by this assumption.

For the ordinary density $\rho(\mathbf{R})=\rho(\mathbf{R}, \mathbf{R})$ beyond α_F, the form (3.17) is not as appealing as it is in the interior region. The arguments associated with Eq. (3.19), applied here, show that at large x the density approaches the classical limit of zero density with $\theta_F^{-2}\exp(-2|\theta_F|)$; that is, the decrease of the nonclassical density is made especially rapid by the fact that there are few waves with k_x near k_F. Just as in the interior, the coefficient of this surviving term depends on the shape of the potential. However in the low-density region it is this coefficient that is of interest, whereas in the high-density region it was sufficient to know that the coefficient was small. For example, in the linear potential treated above,

$$\rho(x)\simeq(\gamma_F^3/16\pi^2)\,(23/1944)\,|\theta_F|^{-2}\exp(-2|\theta_F|),\qquad \text{as } x\rightarrow\infty$$

while for a step potential, the density approaches

$$\rho(x)\simeq(\gamma_F^3/16\pi^2)\,|\theta_F|^{-2}x^{-2|\theta_F|},\qquad \text{as } x\rightarrow\infty.$$

For a potential like that encountered in the nuclear surface, the coefficient will lie in between. In the test case discussed above, at $x=0$ the exact density is not quite twice the value given by the expression derived from a linear potential (3.17).

Therefore the linear potential expression for the local density must be treated skeptically in the region beyond α_F, because it must be expected to underestimate the density in this region. In the numerical work described below, Bethe's recommendation

$$\rho=\rho_2\exp(-2\gamma_F r),\qquad \gamma_F=(-E_F)^{1/2}$$

has been followed, since he examined a fairly realistically shaped potential. ρ_2 has been chosen so that this tail is fit at the classical turning point of the most energetic particle, which occurs at a density of about 0.003 neutrons of protons per fm^3.

V. APPLICATION TO ^{208}Pb

A. Numerical Procedures

A numerical investigation of the procedure described in Sec. IV has been carried out for ^{208}Pb using an electronic computer. The nuclear-matter calculations of Ref. 5 were taken as a basis for this computation. The position-space interaction potential g_c derived there was employed. Its density dependence was approximated as $A(r)+B(r)\rho^{1/3}$ at each value of the relative separation r; the coefficient functions A and B were determined by matching the tabulated potential at $k_F=1.0$ and 1.4 fm^{-1}. The defect integral k was taken as 0.136.

The effective potentials g_c have about 6 MeV too little attraction at saturation. About 2 MeV of this deficiency has been traced[5] to the fact that states of high relative angular momentum $J>2$ are more attractive than predicted by the one-pion-exchange potential, which was used for these states in computing g_c. Much of the remaining attraction has been accounted for as effects of higher-order short-range correlations in Brueckner theory. In order to obtain reasonable numerical results it is necessary to include this attraction in an appropriate manner. This is conveniently done in the present theory by adjusting $W(\rho)$. The adjustment of $W(\rho)$ corresponds to adding a zero-range part of the interaction, of the strength necessary to give the desired nuclear-matter binding. Because the many-body diagrams of Brueckner theory are expected to have a strong density dependence, the adjustment to $W(\rho)$ may also have a strong density dependence. For the numerical work reported here, no additional density dependence was added to $W(\rho)$. Instead, a constant -4.7 MeV was added to each of the five

[14] D. Thouless (to be published).

values of W calculated in Ref. 5. To obtain intermediate values and derivatives, Lagrange interpolation in ρ was used, with an added point $W=0$ at $\rho=0$. The resulting binding-energy curve $W(\rho)$ is shown in Fig. 6.

The symmetry energy was taken as

$$W_S=31\ \text{MeV}(k_F/1.4\ \text{fm}^{-1})^2\beta^2(1-1.7\beta^2),$$

where $\beta=(N-P)/(N+P)$, and k_F is related to $\rho=N+P$. This form and these coefficients were found in Ref. 5. The Coulomb exchange energy was treated in local-plane-wave approximation [$f=1$ in (4.1), but with (4.2) as well]; it was less than -0.4 MeV per proton and so could be crudely approximated.

The density and potential were evaluated at each of 27 radii, varying in 6 steps of approximately 0.8 fm and then in 20 steps of about 0.3 fm. The intervals were chosen so that the last point of the radial mesh occurred at the classical turning point for the most energetic neutron; below this density, as remarked above, an exponential tail was used. For the protons, the tail's decay constant was $\gamma_p=(C-E_p)^{1/2}$, where C was the Coulomb potential at the last radius treated; the proton tail was fit at the classical turning point corresponding to the proton Fermi energy E_p. The potentials U^D and U^X were transformed into integrals over the relative coordinate $\mathbf{r}-\mathbf{r}'$, which were evaluated by Simpson's rule. The integrands were evaluated at 41 values of the cosine of the angular coordinate and 79 values of the radial coordinate (21 values from 0.05 to 1.05 fm, them in larger steps to 6.85 fm).

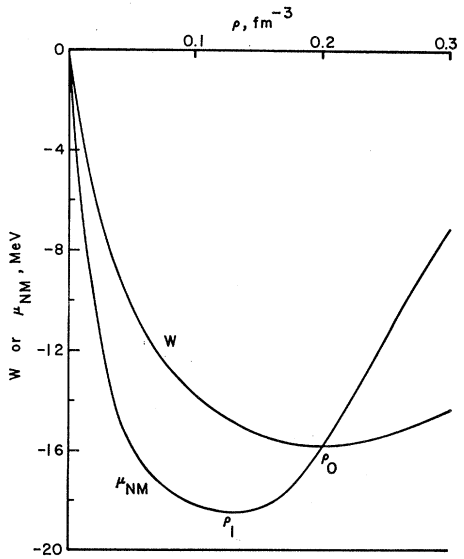

FIG. 6. Nuclear-matter binding energy per particle $W(\rho)$, and chemical potential $\mu_{\rm NM}(\rho)=\partial/\partial\rho(\rho W)$. The results of Ref. 5 have been augmented by -4.7 MeV per particle, except at $\rho=0$.

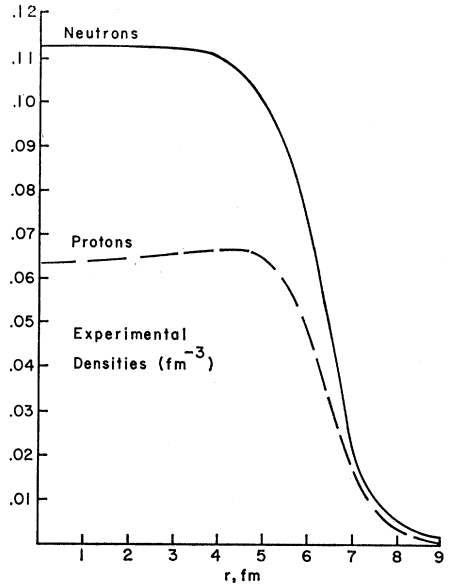

FIG. 7. Density distributions in ^{208}Pb inferred from experiment. Proton density from Ref. 15. Neutron density from Ref. 16.

B. Potentials for Experimental Densities

The potentials $U_n(\mathbf{r})$ and $U_p(\mathbf{r})$ were calculated for the experimentally inferred density distributions of protons[15] and neutrons,[16] which are reproduced in Fig. 7. To find a potential from a density distribution, it is necessary to know the wave-number integrals z_n and z_p [Eq. (4.9)], which are integrals of the potential being computed. Therefore a guess at the potential was made in order to begin the calculation; its wave-number integrals were used to calculate a new potential, and so on until the potential was roughly self-consistent as indicated by the fact that it did not change from iteration to iteration at any point by more than about 2% of its value near the center of the nucleus. The neutron and proton Fermi energies were estimated by their removal energies of -7.375 and -8.034 MeV, respectively[17]; they should be somewhat more negative because of rearrangement effects.

The resulting single-particle potentials for the experimental density distributions are shown in Fig. 8. Figure 9 shows the local nuclear-matter potentials $\partial(W^*\rho)/\partial N$ and $\partial(W^*\rho)/\partial P$, and the Coulomb potential seen by the protons. The inhomogeneity corrections U^D and U^X are graphed in Fig. 10.

C. Role of U^X in the Surface

Special attention is due the inhomogeneity correction U^X arising from the space-exchange force. In

[15] J. B. Bellicard and K. J. van Oostrum, Phys. Rev. Letters **19**, 242 (1967). The distribution used is their fit with $w=0.14$.

[16] H. A. Bethe and P. J. Siemens, Phys. Letters **27B**, 549 (1968).

[17] J. H. E. Mattauch, W. Thiele, and A. H. Wapstra, Nucl. Phys. **67**, 1 (1965).

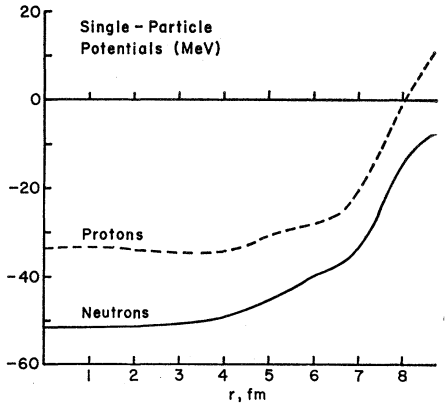

FIG. 8. Single-particle potentials U_n (solid curve) and U_p (dashed curve) resulting from experimental density distributions, according to Eq. (4.7).

the surface it is as large as the inhomogeneity correction U^D due to the ordinary (direct) force, though it disappears more rapidly in the interior. Previous theories have taken account of only U^D.

Because the present theory's expression for the density so rapidly approaches the Thomas-Fermi expression, the discussion of Sec. II D applies to it as well. There it was shown that, because of a condition on the derivatives of the potential at the point where the density reaches the minimum ρ_1 of the nuclear-matter chemical potential, a theory with only the direct-force inhomogeneity term U^D has no possibility of giving a reasonable density distribution. The exchange correction U^X, however, revives hope for the theory, because it has a positive derivative in the region of the "shoulder" of the density distribution. This positive derivative is just what is needed to meet the objection of Sec. II D.

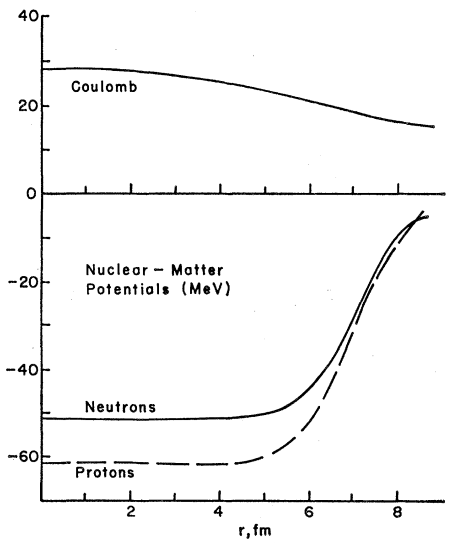

FIG. 9. Contributions to single-particle potentials due to derivative of local nuclear-matter energy density, $\partial(W\rho^*)/\partial N$ (solid curve) and $\partial(W\rho^*)/\partial P$ (dashed curve).

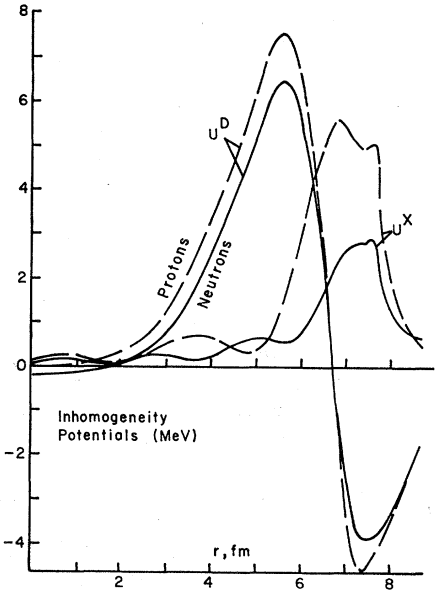

FIG. 10. Inhomogeneity corrections to single-particle potentials of neutrons (solid curves) and protons (dashed).

Thus the beginning of the rise of U^X must be closely correlated with the place at which the density passes through ρ_1. The critical nature of this correlation makes the model very sensitive to the properties of g and W. If either g or W is changed, the wave-number integrals will also change, which can strongly affect the size and position of the maximum of U^X.

The g and W investigated here do not make U^X quite large enough where the density passes through ρ_1. As a result, when densities are calculated in the potential of the experimental distribution, they have

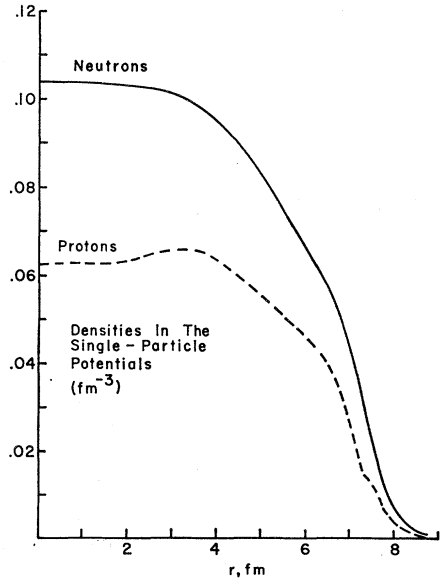

FIG. 11. Density implied by Eqs. (3.14)–(3.16) from potentials of Fig. 8.

about 0.3 fm too large a half-density radius, as Fig. 11 shows. Also, the proton eigenvalue $E_p=-2.51$ MeV is incorrect, though $E_n=-7.97$ MeV is approximately right. When the potential U^X is calculated from the new distribution of Fig. 11, both the large radius and the high proton Fermi energy help to move the peak of U^X to a still larger radius. This makes it harder to satisfy the condition of Sec. II D. It also makes the density distribution of the next iteration have a still larger radius. Thus the procedure does not converge for the forces used.

VI. DISCUSSION

Because the Thomas-Fermi theory does not include enough of the physics of wave functions, it fails as a nuclear model in two ways. First, because it does not allow the wave functions to anticipate their classical turning points, it has singular solutions. Second, because it has an inadequate treatment of the space-exchange contribution to the potential energy, its continuous solutions could never rise to a sufficient central density to take advantage of the full binding of nuclear matter. Both these failures are remedied by the model developed in Sec. IV, which uses approximate wave functions.

The new statistical model is sensitive to the force and to the nuclear-matter saturation curve employed. The exchange inhomogeneity correction U^X is especially sensitive to the low-density region, because the phase integrals z_n and z_p emphasize the region near the last classical turning point. The size of the potential U^X is very sensitive to z, because U^X depends on the product of the rapidly varying factor ρ^2 and $(1-F^2)$. The latter of these factors contains an oscillatory component; the position of its peak relative to the decrease of ρ^2 determines the magnitude of the peak of U^X. The resulting sensitivity to the shape of W at low density is disconcerting because W is not well known in this region. This sensitivity is probably an artificial feature of the model. Since the model is so sensitive to U^X, it may not have been justifiable to neglect the variation of z_n and z_p in constructing Eq. (4.9) for U^X. Perhaps if this variation were taken into account, the behavior of U^X would be made less critical.

It is not clear whether the disappointing numerical results of Sec. V are to be blamed on the statistical model or on the interaction of Ref. 5. Particularly puzzling is the excessively large difference in proton and neutron potentials near the center of the nucleus, which is undoubtedly responsible for the poor proton eigenvalue. Some difference between neutron and proton potentials is to be expected, because the symmetry energy attraction will not completely compensate for the Coulomb repulsion felt by the protons. But the difference shown in Fig. 8 is unexpectedly large.

It is encouraging that the central proton density of the inferred charge distribution (Fig. 11) is about right. Probably the neutron density is also acceptable, since a recent improvement in the measurement of the isobaric analog energy[18] implies that the neutron surface should be about 0.1 fm farther out than it is in the distribution cited above. Thus in the interior region, the experimental density is nearly self-consistent. This seems to indicate that the saturation density of W is correct as used here, that is, without additional density dependence from higher-order diagrams.

It is not certain that the normalization conditions are sufficient to determine the Fermi energies E_n and E_p. Since the new model is asymptotic to the Thomas-Fermi model in the interior of the nucleus, it is also vulnerable to the argument that the interior region cannot determine the Thomas-Fermi eigenvalue. The reason for this is that in the interior, the inhomogeneity terms U^D and U^X vanish; thus the Thomas-Fermi equation becomes merely

$$E_F=\mu_{\mathrm{NM}}[\rho(\mathbf{r})].$$

There will be at least one density ρ which satisfies this equation for any E_F greater than the minimum value of μ_{NM}. Nor does the normalization condition help, for if a solution of a given surface shape and interior density has the wrong number of particles, a new solution with the desired norm can be obtained by shifting the surface radius in or out, changing the volume of the uniform-density interior region till the nucleus contains the right number of particles. Perhaps the stringent requirements on the region near the minimum of μ_{NM} are sufficient to fix the eigenvalues; but if that is the case, then the central density is determined by a surface condition, which is an unacceptable circumstance in the limit of a very large nucleus.

Thus it appears that there remains a degree of freedom in the statistical model, associated with the choice of the Fermi energy E_F. This added degree of freedom was removed in the Thomas-Fermi model by Bethe's observation that the eigenvalue must equal the energy per particle. A corresponding condition is lacking in the new model. If, in fact, the Fermi energies are not sufficiently determined, then the numerical behavior of the theory has good cause to be puzzling.

ACKNOWLEDGMENTS

I am grateful for the constant encouragement and advice of Professor Hans Bethe, and for many helpful conversations with Dr. Baird Brandow and Dr. John Negele.

[18] G. H. Lenz and G. M. Temmer, Nucl. Phys. A112, 625 (1968). Dr. J. Jänecke has pointed out these newer data.